

NMR-Driven Discovery of Benzoylanthranilic Acid Inhibitors of Far Upstream Element Binding Protein Binding to the Human Oncogene *c-myc* Promoter

Jeffrey R. Huth,[†] Liping Yu,[†] Irene Collins,[‡] Jamey Mack,[†] Renaldo Mendoza,[†] Binumol Isaac,[†] Demetrios T. Braddock,[§] Steven W. Muchmore,[†] Kenneth M. Comess,[†] Stephen W. Fesik,[†] G. Marius Clore,[#] David Levens,[‡] and Philip J. Hajduk^{*,†}

Global Pharmaceutical Research and Development, Abbott Laboratories, 100 Abbott Park Road, Abbott Park, Illinois 60064, Laboratory of Pathology, National Cancer Institute, National Institutes of Health, Bethesda, Maryland 20892, Department of Pathology, 404A Lauder Hall, Yale School of Medicine, New Haven, Connecticut 06520-8023, and Laboratory of Chemical Physics, National Institute of Diabetes and Digestive and Kidney Diseases, National Institutes of Health, Bethesda, Maryland 20892

Received March 19, 2004

Reversal of aberrant gene expression that is induced by the proto-oncogene *c-myc* is likely to be effective for treating a variety of tumors that rely on this pathway for growth. One strategy to down-regulate the *c-myc* pathway is to target transcription factors that regulate its own expression. A host of proteins act in coordination to regulate *c-myc* expression and any one of them are theoretical targets for small-molecule therapy. Experimentally, it has been shown that the far upstream element (FUSE) binding protein (FBP) is essential for *c-myc* expression, and reductions in FBP levels both reduce *c-myc* expression and correlate with slower cell growth. FBP binds to ssDNA by capturing exposed DNA bases in a hydrophobic pocket. This suggests that a small molecule could be designed to occupy this pocket and inhibit FBP function. Using a variety of screening methodologies, we have identified ligands that bind to the DNA binding pockets of the KH domains of FBP. Gel shift analyses using full length FBP and a related transcription factor confirm that a small-molecule lead compound inhibits DNA binding in a specific manner. The benzoylanthranilic acid compounds described here represent leads in the design of FBP inhibitors that can serve as useful tools in the study of *c-myc* regulation and in the development of therapeutics that target the *c-myc* pathway.

1. Introduction

Disruptions in the regulation of the *c-myc* proto-oncogene are some of the most common genetic abnormalities associated with cancer.¹ Because of this central role in tumor progression,² the *c-myc* pathway remains a sought-after target for small-molecule therapy of solid tumors. While in principle the c-Myc protein could be targeted directly with a small-molecule antagonist, this has proven to be difficult. Disruption of the helix–loop–helix leucine zipper interaction with DNA is not easily achieved with a small molecule because a pocket suitable for small-molecule binding is not apparent on the c-Myc DNA binding domain. Alternatively, interference with the trans-activating domain could result in suppression of tumor growth. As the interacting proteins with c-Myc become better understood,³ inhibition of the downstream effectors of c-Myc may yield potent therapeutics. An alternative approach is to modulate the upstream pathways that control *c-myc* expression. One protein that plays a pivotal role in the *c-myc* transcription is the far upstream element (FUSE) binding protein, otherwise known as FBP. FBP binds to single-stranded DNA ~1500 base pairs upstream of the *c-myc* gene and is involved in activating the helicase activity of TFIIH (Figure 1).⁴ A working hypothesis is that the

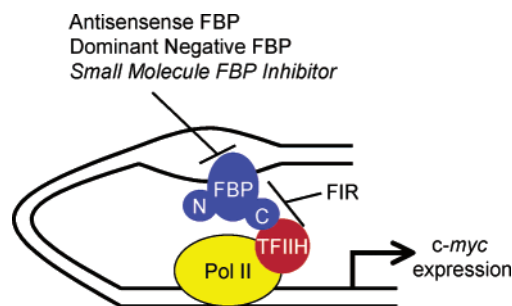


Figure 1. Proposed mechanism for inhibition of c-Myc mediated cell growth by targeting FBP. FBP increases transcription of the *c-myc* gene by enhancing the ability of TFIIH to release paused RNA polymerases.⁴ When overexpressed in tumor cells, the c-Myc protein participates in global transcriptional regulation by modulating the expression of hundreds of genes, many of which are involved in cell growth and malignant transformation.⁴³ This is counteracted by FIR, which binds to both FBP and TFIIH and down-regulates the TFIIH helicase activity.⁹ Pharmacological control of aberrant *c-myc* expression is suggested by the ability of antisense FBP RNA and a dominant negative FBP protein to inhibit *c-myc* expression.⁵ This suggests that targeting FBP with a small molecule and inhibiting its binding to ssDNA would also inhibit *c-myc* expression and tumor cell growth.

release of paused RNA polymerases downstream of the *c-myc* promoter is regulated by TFIIH. Thus, the role of FBP may be to regulate the rate-limiting step in *c-myc* expression by modulating the transition from transcription initiation to promoter escape.⁵ Evidence for this dominant role in controlling *c-myc* expression comes

* To whom correspondence should be addressed. Phone: (847) 937-0368. Fax: (847) 938-2478. E-mail: philip.hajduk@abbott.com.

[†] Abbott Laboratories.

[‡] National Cancer Institute.

[§] Yale School of Medicine.

[#] National Institute of Diabetes and Digestive and Kidney Diseases.

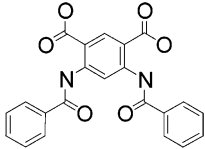
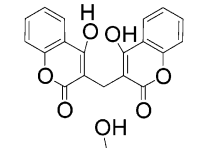
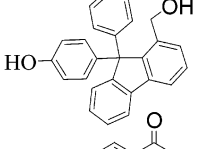
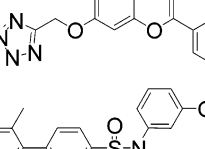
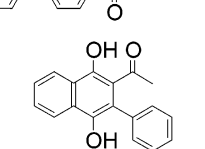
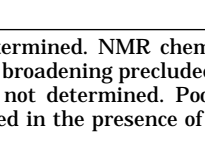
from knockout experiments. The expression of a dominant-negative FBP or antisense FBP RNA down-regulated *c-myc* expression and arrested cellular proliferation (Figure 1).⁵ These experiments suggest that disruption of FBP function with a small molecule could inhibit the proliferation of *c-Myc* dependent tumors.

FBP consists of 658 amino acids organized in N-terminal, central, and C-terminal domains. The N-terminal repression domain⁵ contains a predicted amphipathic helix,⁶ while the C-terminal domain imparts the trans-activating activity of FBP via a tyrosine-rich region.^{6,7} Regulation of FBP protein levels seems to be mediated by the C-terminal domain where p38 binds and stimulates FBP degradation via ubiquitination.⁸ Further regulation of FBP function occurs at the central DNA binding domain. This consists of four tandem K homology (KH) repeats and is the site for binding of the FBP interacting repressor (FIR).⁹ Through this interaction, FIR interacts with TFIID and down-regulates its helicase activity. KH3 and KH4 of FBP are sufficient to impart binding to bases -1525 to -1553 of the *c-myc* gene.⁷ The NMR structure of a complex between the KH3/KH4 repeats of FBP and single-stranded (ss) DNA¹⁰ shows that two helices, the GXXG loop, and a β strand form a groove to which the ssDNA binds. The center of this groove is hydrophobic and interacts with the exposed bases of the ssDNA. The sugar-phosphate backbone binds to the more polar edges of the FBP groove. These structural characteristics of the DNA binding site distinguish FBP from the more common transcription factors that bind to double-stranded DNA, where the pocket involved in the interaction is either the DNA major or the DNA minor groove. Although compounds have been developed to bind to DNA,¹¹ achieving binding specificity is still a major challenge. For ssDNA binding transcription factors such as FBP, the protein forms the binding pocket, making this type of transcription factor more attractive from a drug design point of view. In this report, we describe the use of NMR-based screening for identifying small molecules that bind to FBP. On the basis of structural studies, we show how a novel small-molecule FBP ligand inhibits DNA binding of FBP by targeting its ssDNA binding pocket.

2. Results and Discussion

Lead Identification. Both the KH3 and KH4 domains of FBP adopt stable folds and can independently bind to ssDNA.¹⁰ The mode of binding is similar with a hydrophobic cleft accommodating the exposed bases of the DNA. *A priori* it was not clear which KH domain would be most amenable to inhibition by a small molecule. As a result, we chose to screen a tandem construct that included both the KH3 and KH4 domains, hereafter termed FBP3/4. Three approaches were undertaken to identify potential ligands: (1) HTS-NMR,¹² (2) virtual ligand screening (VLS),¹³ and (3) affinity selection/mass spectrometry (ASMS).¹⁴⁻¹⁶ By use of HTS-NMR, a library of 105 000 small molecules was screened that resulted in three ligands for FBP3/4 (Table 1). By use of the program FRED, 584 000 compounds from the Abbott corporate collection were screened *in silico*, and the best 103 compounds were tested at 0.5 mM for binding to FBP3/4 by NMR. This

Table 1. Leads Ligands for FBP3/4

Compound	Structure	NMR K_D	Screen
1		0.35 mM	HTS-NMR
2		-- ^a	HTS-NMR
3		-- ^a	HTS-NMR
4		1.7 mM	VLS
5		-- ^a	VLS
6		-- ^b	ASMS

^a (-) not determined. NMR chemical shift changes were observed, but line broadening precluded the ability to measure a K_D by NMR. ^b (-) not determined. Poorly Soluble. No NMR shift changes observed in the presence of 0.1 mM compound.

yielded an additional two leads (Table 1). A subset (240 000) of the compounds screened *in silico* was screened by ASMS, and one was found to bind to FBP3/4 (Table 1). Interestingly, the three hits identified via NMR were in the VLS library but were not ranked in the top 1000 compounds. However, an analogue of **1** was ranked in the top 0.1% (374 of 584 000). All of the NMR and VLS hits were in the library screened by ASMS, but their weak affinity precluded detection using this technique.

Compounds **1-5** were found to bind to the same site on FBP3/4, as evidenced by similar patterns of chemical shift changes (data not shown). As shown in Figure 2, the largest chemical shift changes map to the DNA binding site of the KH3 domain. Chemical shifts for corresponding residues in the KH4 domain could not be determined because of line broadening of these peaks in uncomplexed FBP3/4. Not surprisingly, all of the compounds contain acidic moieties that may mimic the phosphate backbone of single-stranded DNA and interact favorably with the positively charged residues on FBP3/4. For example, compound **1** contains two carboxylic acid groups, while compound **4** contains a tetrazole group that can serve as an isostere for a carboxylate. The remaining compounds all contain one or more phenolic oxygens that are also acidic and can interact with basic residues.

Structural Studies and SAR. To more accurately determine the mode of binding, NOE studies were

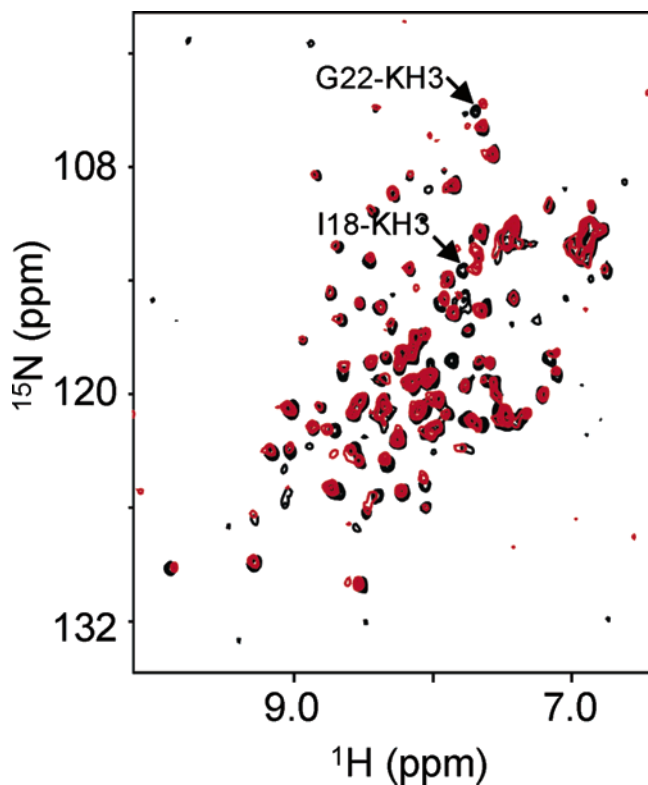


Figure 2. 2D ^1H - ^{15}N HSQC spectra of FBP3/4 in the absence (black) and presence (red) of 1 mM compound **4**. Arrows indicate the largest chemical shift changes (G22 and I18 in the DNA binding pocket of the FBP3 domain).

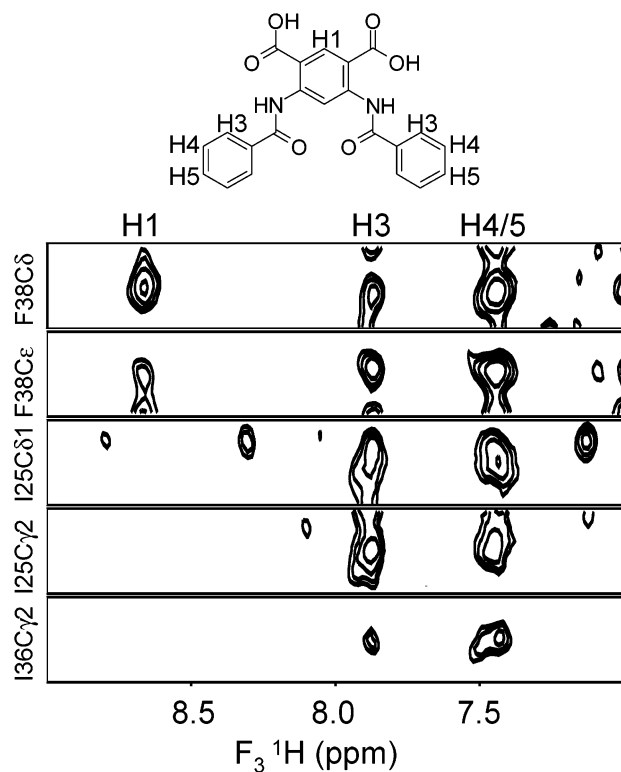


Figure 3. Strips from a 3D ^{13}C -separated/ ^{12}C -filtered NOE experiment illustrating intermolecular NOEs between protein protons attached to ^{13}C and protons of the benzoylanthranilic acid of **1** attached to ^{12}C (along the F_3 axis). Protein assignments are indicated to the left, and ligand assignments are along the top of the NOE strips.

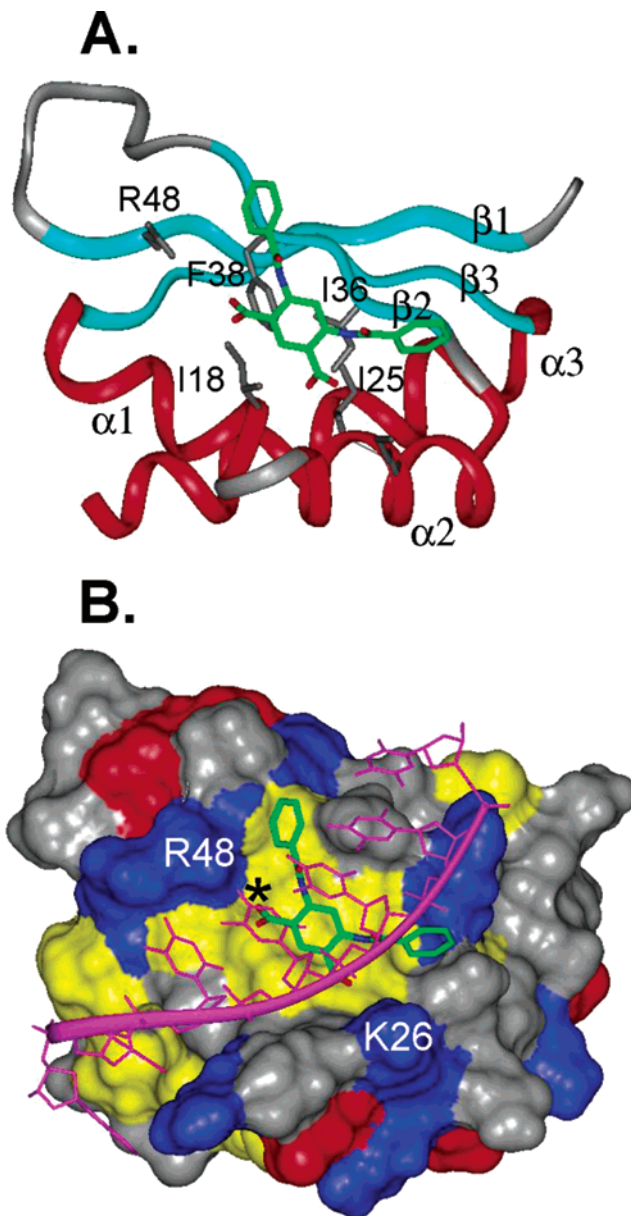
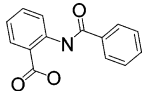
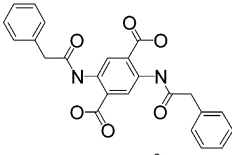
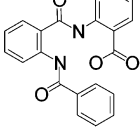
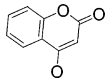


Figure 4. (A) Ribbon diagram depicting the KH3 domain in complex with compound **1** (rendered and colored by atom type). The α -helices, β -strands, and loops are shown in red, cyan, and gray, respectively. (B) Connolly surface of the KH3 domain of the KH3/compound **1** (green carbon atoms) complex overlaid with the ssDNA substrate (magenta) observed in complex with the KH3 domain.¹⁰ Positively and negatively charged residues are colored in blue and red, respectively, while the hydrophobic residues Ile, Leu, Val, Met, and Phe are colored in yellow (all other residue types are in gray). The O4 atom of the thymidine base that overlaps with one carboxyl of compound **1** is identified with an asterisk.

performed on a complex of compound **1** and the KH3 domain of FBP. NOEs from the ligand to Ile 18, Ile 25, Ile 36, and Phe 38 of the protein (Figure 3) confirmed that the ligand binds to the ssDNA binding site. By use of 28 intermolecular NOEs, compound **1** was docked onto FBP3 keeping the protein backbone and side chains fixed during the calculation. A family of structures with no intermolecular NOE violations was averaged to construct the NOE-based model shown in Figure 4. This NOE-based model shows that the ligand binding surface is composed of helices α_1 and α_2 as well as the β_2 strand (Figure 4A). The central ring of the ligand lies against

Table 2. Inhibition Activity of Structural Analogues of Compound **1**

Compound	Structure	NMR K_D
7		>4 mM
8		1 mM
9		0.6 mM
10		— ^a

^a A control for the gel shift experiments for which no chemical shift changes are observed by NMR in the presence of 0.5 mM ligand.

the hydrophobic surface of the protein with the carboxylate groups potentially interacting with the positively charged side chains of Lys26 and Arg48 (Figure 4B). The outer rings of the ligand pack against two hydrophobic pockets on the protein surface. A comparison with the ssDNA complex shows that compound **1** occupies the central, most hydrophobic region of the DNA binding pocket (Figure 4B). Orientation of the ligand in this pocket seems to be directed by polar interactions on either side of the pocket that mimic naturally occurring interactions with the T nucleotides of ssDNA. In particular, one carboxylate group of the ligand mimics the phosphate group of the ssDNA while the other carboxylate group mimics the O4 atom of one T nucleotide (indicated with an asterisk). It was expected on the basis of this structure that compound **1** would interfere with substrate binding by preventing the interactions of the central DNA bases in the core FBP recognition sequence.

To explore the SAR for the benzoylanthranilic acid inhibitors, structural analogues were analyzed for binding to the FBP3/4 construct. While no compounds could be purchased that were at least 85% similar to compound **1** or that contained the substructure of this lead, 16 structural analogues were obtained from our corporate compound collection with similarity values of 46–84%. The results of a subset of these are shown in Table 2. Removal of one benzamide moiety (compound **7**) completely abrogated binding to FBP3/4, indicating that both benzamide groups of compound **1** are critical for binding to FBP. That the compound is symmetric but the binding surface of FBP3 is not symmetric clearly provides avenues for improvements in potency. This is supported by the SAR in that the relative orientations of the aromatic amide moieties can vary. For example, compound **8** contains benzyl groups linked in a para orientation from the central phenyl ring, whereas in compound **1** this orientation is meta. However, both compounds bind to FBP3 with comparable affinities.

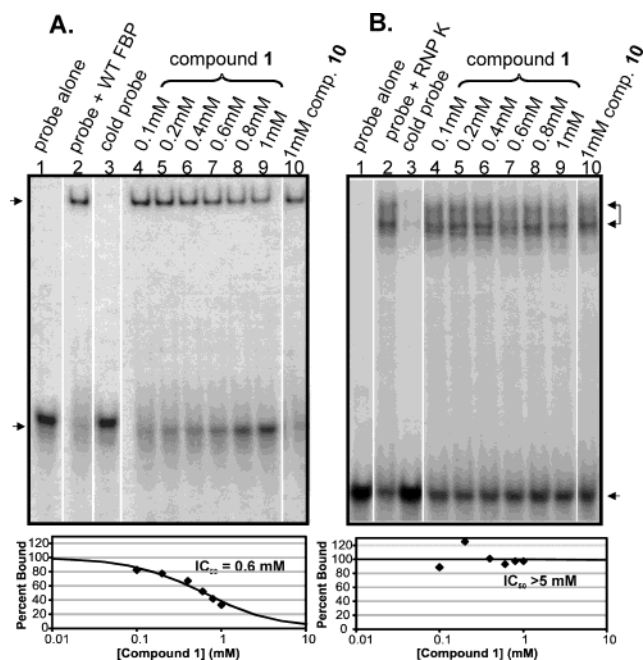


Figure 5. Gel shift assays in the presence and absence of compound **1** and the inactive control, compound **10**. Arrows indicate the positions of the protein–DNA complex (upper arrow) and free probe (lower arrow). (A) (lane 1) 0.1 pmol of labeled FMYC 1-6 oligo, which represents the FBP binding site within the FUSE element;⁴¹ (lane 2) 0.1 pmol of labeled probe with 0.1 pmol of insect cell expressed HIS tagged full length FBP; (lane 3) FBP/labeled probe complex + 10 pmol of unlabeled probe; (lanes 4–10) FBP/labeled probe complex + small molecules as indicated. (B) (lane 1) 0.1 pmol of labeled EM 8 oligo, which represents the hnRNP K binding site;⁴² (lane 2) 0.1 pmol of labeled probe with 0.2 pmol of bacterially expressed GST-human RNP K; (lane 3) RNP K/labeled probe complex + 0.5 pmol of unlabeled probe; (lanes 4–10) RNP K/labeled probe complex + small molecules as indicated. Multiple bands for the bound RNP K probe bound to GST-RNP K and GST-cleaved RNP K have been previously observed.⁷ Graphs below the gels include densitometry measurements for the complexes as a function of compound **1** concentration. A least-squares fit of the data for FBP yielded an estimated IC_{50} of 0.6 mM. No inhibition of binding to RNP K was detected at up to 1 mM compound **1**.

This suggests that one-half of the small-molecule ligand contributes very weak and unoptimized interactions to the overall binding. Compound **9**, which contains only a single acid, binds to FBP3/4 with a K_D of 0.6 mM, suggesting that only one acid is required for binding.

Gel Shift Assays. To demonstrate that a small molecule can inhibit the function of FBP, compound **1** and an inactive control (compound **10**) were analyzed for their ability to disrupt FBP binding to the *c-myc* promoter. Compound **1** clearly inhibited binding of the DNA probe to His-tagged full length FBP, whereas the negative control compound did not (Figure 5A). In addition, titration results demonstrated that the IC_{50} of compound **1** for inhibiting probe binding is comparable to the K_D value of 0.35 mM observed by NMR (Table 1). A least-squares fit of densitometry data yielded a dissociation constant of 0.6 mM (Figure 5A). Binding of compound **1** to the KH domain of FBP also seems to be at least moderately specific. In high-throughput screens of 78 drug targets at Abbott Laboratories, compound **1** failed to inhibit any target with $IC_{50} < 100 \mu M$ (Dr. James Kofron, personal communica-

tion). Furthermore, the compound was ineffective ($IC_{50} > 5$ mM) in inhibiting DNA binding of the GST-tagged hnRNP K protein (Figure 5B), which contains structurally homologous KH domains with different ssDNA sequence specificities.¹⁷

Implications for Small-Molecule Inhibition of FBP. The leads derived from these screening exercises represent important starting points that encourage further research. While cellular activity of these compounds could not be assessed because of insufficient solubility in the cell growth medium, the observation that compound **1** inhibits FBP *in vitro* by binding to the KH3 domain suggests that a more potent analogue in this series would exhibit efficacy in cell culture. Indeed, antisense FBP RNA both down-regulates transcription of probe molecules driven by the *c-myc* promoter and inhibits *c-Myc* dependent growth of cells in culture (summarized in Figure 1).⁵ The results presented here indicate that a small molecule could accomplish the same level of cellular activity given sufficient potency and cell permeability.

From a drug design perspective, inhibiting a protein–DNA interaction shares many similarities to inhibiting protein–protein interactions, which also contain large interaction surfaces. In practice, it can be challenging to find potent inhibitors of protein–DNA or protein–protein interactions from high-throughput screening.^{18,19} A major factor contributing to this phenomena is that a significant fraction of compounds that comprise corporate repositories have been designed to inhibit enzymes and GPCRs. Thus, many protein–protein or protein–DNA interactions may in fact be druggable; it is simply that appropriate lead compounds cannot be found because they do not exist.²⁰ Many literature examples exist to support this claim, including inhibitors of the HPV-E2/DNA complex,²¹ where fragment-based approaches to drug discovery succeeded in producing leads where HTS failed, and the recently reported potent inhibitors of the IL-2/IL-2R α complex,²² after decades of unproductive HTS campaigns.²³ The fact that no close structural analogues of compound **1** exist in our internal or commercial repositories highlights the fact that new chemical space must be explored in order to effectively inhibit these novel protein targets. Another lesson that can be gleaned from inhibitors of protein–protein interactions is that protein targets that have high potential for drug development tend to be temporary complexes²⁴ that have binding “hot spots” that impart the majority of the binding energy.^{25,26} Given these criteria and the work presented here, FBP clearly has potential for therapeutic intervention because it forms only a temporary complex with its cognate DNA and contains a “hot spot” at the DNA-binding interface that can bind to small molecules and disrupt its biochemical function.

Lead Optimization Strategies. Multiple avenues exist for improving potency of the benzoylanthranilic acids. High-resolution structures of FBP/ligand complexes could be utilized in structure-based design efforts to improve potency. As shown in Figure 4B, the central phenyl ring of **1** lies against a large hydrophobic surface. This structure indicates that more extensive hydrophobic contacts could be achieved with additional ring substitutions. Also, the model suggests that the protein

interactions with one of the outer rings of **1** differ from those made by the sugar–phosphate backbone of ssDNA. This suggests that alternative ring systems that more closely mimic the interactions afforded by a DNA backbone may improve the potency of benzoylanthranilic acid inhibitors. The presence of an amide bond linking the rings of compound **1** opens up the possibility for combinatorial chemistry approaches to rapidly address this question.

An alternative way to improve potency is to take advantage of the modular arrangement of KH domains in FBP. As has been shown for other systems, tethering two low-affinity ligands can result in highly potent compounds.^{27–29} Thus, linking ligands for the KH3 and KH4 domains of FBP using an appropriate tether could result in highly specific and potent inhibitors of this transcription factor. This is supported by the fact that each KH domain independently binds to ssDNA with only micromolar affinities, while the tandem KH3/KH4 construct exhibits nanomolar affinity.¹⁰ This modular chemical approach to inhibit transcription factor activity is not without precedence. Dervan and colleagues have developed polyamide compounds that recognize the minor groove of specific DNA sequences.³⁰ Antiparallel dimers of polyamides in which five-membered heterocycles are connected by amide linkages form an arch-shaped structure that fits the curvature of the minor groove and interacts with specific DNA base pairs via hydrogen bonding. Chemically linking two polyamides improves the affinity of these polyamides to subnanomolar levels. Significantly, polyamide dimers have been shown to access the nucleus in cell culture and modulate transcription.³¹ In an analogous fashion, appropriately tethered dimers of ligands for FBP represent a complementary way to inhibit transcription *in vivo* by binding to the transcription factor protein rather than to the DNA promoter.

3. Conclusions

In summary, the benzoylanthranilic acids described here represent novel leads that specifically target the DNA binding domain of FBP and that inhibit the enhancer activity of this transcription factor at the *c-myc* promoter. Structure-guided improvements in the potency of this series may lead to inhibitors of FBP/DNA binding that can be important tools in the study of *c-myc* regulation and in the development of therapeutics that target the *c-myc* pathway.

4. Experimental Section

Preparation of FBP. The individual KH3 and tandem KH3/KH4 domains of human FBP, residues 278–350 and 278–447, respectively, were cloned into pET 15b and expressed in *E. coli* BL21(DE3) cells as previously described.¹⁰ For NMR screening studies, FBP3/4 was labeled with ¹³C at the methyl groups of valine and leucine and the δ -methyl of isoleucine by including [¹³C]- α -ketobutyrate and [3,3'-¹³C]- α -ketoisovalerate in the medium.³² FBP3/4 was purified by nickel affinity chromatography, stored in sodium phosphate buffer, pH 7.0, 500 mM NaCl, 20 mM imidazole, 2 mM DTT at 4 °C, and transferred to 50 mM sodium phosphate buffer, pH 7.0, 100 mM NaCl, 20 mM imidazole, 2 mM DTT for NMR screening experiments. For structural studies, FBP3 was uniformly labeled with ¹⁵N and ¹³C by growing the cells on ¹⁵N ammonium chloride and ¹³C glucose. This protein was purified as described.¹⁰

NMR Screening and Titrations. NMR samples comprised ^{13}C -methyl-labeled FBP3/4 at 25 μM in a $\text{H}_2\text{O}/\text{D}_2\text{O}$ (9:1) buffer as described above. Ligand binding was detected at 30 $^\circ\text{C}$ by acquiring ^1H - ^{13}C heteronuclear single quantum correlation (HSQC) spectra in the presence and absence of compounds. Compounds were initially tested at 50 μM each in mixtures of 100, with subsequent deconvolution to mixtures of 10 at 50 μM each, and then to individual compounds. Spectra were acquired in 15 min with 38 complex points on Bruker 500 MHz spectrometers equipped with cryoprobes. Chemical shift mapping of the binding site for compound **4** was achieved by measuring ^{15}N chemical shifts of 0.1 mM labeled FBP3/4 in the presence of 1 mM compound and comparing the shifts to the backbone chemical shift assignments. Free FBP3/4, uniformly labeled with $^{13}\text{C}/^{15}\text{N}$, was assigned using conventional 3D triple resonance experiments.³³ Dissociation constants were obtained for selected compounds by monitoring the ^{13}C chemical shift changes as a function of ligand concentration. Data were fit using a single-binding site model. A nonlinear least-squares optimization was performed by varying the values of K_D and the chemical shift of the fully saturated protein.³⁴

Virtual Ligand Screening. A total of 584 000 compounds from the Abbott Laboratories corporate compound collection were used as the source library for virtual screening experiments. The target structure for the virtual screening work was the complex of FBP3 with ssDNA.¹⁰ In preparation for the screening exercise, the ssDNA portion of the complex was removed, leaving the binding site exposed. All docking calculations were undertaken with the OpenEye Software, Inc. suite of programs (<http://www.eyesopen.com/index.html>). Conformer libraries were calculated using OMEGA, with an average of 135 conformers generated per molecule of the input library. VIDA, a visualization program, was used to set up the boundary conditions on the protein and to inspect the subsequent docking results. FRED was used to undertake the actual docking calculations. Docking calculations using the Chemscore,³⁵ Screenscore,³⁶ and Gaussian shape-based¹³ functions were compared, and 103 of the top scoring compounds were selected on the basis of visual inspection of their predicted orientation with respect to the FBP structure.

ASMS Screening. Affinity screening¹⁴ of our corporate compound repository was carried out by allowing candidate binders to reach equilibrium with the FBP3/4 protein construct in solution, separating binders from nonbinders using a filtration step, and then directly identifying the binders by mass spectrometry. Large mixtures of compounds at 1.5 μM each compound were allowed to interact with protein at 10 μM for 40 min, and the nonbinders were separated by ultrafiltration using a 10 kDa molecular weight cutoff regenerated cellulose membrane (Microcon concentrator, Millipore, Bedford, MA). Approximately 240 000 compounds from the Abbott corporate collection were screened in duplicate. The retentates were treated with methanol and methylene chloride to denature the protein and extract the small-molecule binders. These compounds then were identified by flow injection mass spectrometry by using electrospray ionization (Waters LCT, Milford, MA) and Abbott proprietary analysis software.

NMR Structural Studies. NMR spectra were collected at 30 $^\circ\text{C}$ on a Bruker DRX500 or DRX800 NMR spectrometer. The 2D ^{12}C -filtered and 3D ^{13}C -separated/ ^{12}C -filtered NOE spectra^{33,37} and ^{13}C -separated NOE spectra³⁸ were collected with mixing times of 100 and 150 ms on samples comprising 0.9 mM FBP3 and 2.0 mM compound **1**. The chemical shift assignments for compound **1** were made using a combination of COSY, TOCSY, HMQC, HMBC, and ROESY experiments. The intermolecular NOEs between the ligand and the protein were assigned on the basis of the previous assignments of the free FBP protein as well as 3D ^{13}C -separated NOE and HCCH-TOCSY spectra of the current FBP/ligand complex. The protein/ligand complex structure was generated by using the previously published KH3 domain structure¹⁰ and by docking the ligand onto the protein based on 28 intermolecular NOE restraints³⁹ to the DNA binding site using Xplor-NIH.⁴⁰ Additional NOEs to residues 2, 4, 34, 35, and 53 were also

observed indicating that compound **1** also binds to a second site near the N-terminus. However, at ligand concentrations below 1 mM, very small or no backbone amide chemical shifts are observed for residues in this pocket, indicating much weaker binding than to the DNA binding site. Thus, NOEs to these residues were not included in the structure calculations. The KH3 protein (including the protein side chains) was treated as a rigid body, and the ligand was allowed to freely rotate under the influence of intermolecular NOEs except for maintaining planarity of the aromatic rings and trans-amide bond conformations during the docking. The intermolecular NOEs that could not be assigned to a specific proton on compound **1** because of chemical shift degeneracy of the aromatic rings A and C (Table 1) were incorporated in the structure calculations by using ambiguous NOE restraints. Distances for these aromatic ring protons were represented as a $(\sum r^{-6})^{-1/6}$ sum.

Gel Shift Assays. Full length His-tagged FBP was expressed in baculovirus-infected insect cells and purified as described.⁵ The gel shift reaction buffer consisted of 25 mM HEPES, 100 mM NaCl, 0.2 mM EDTA, 1 mg/mL BSA, 1 mM DTT, 50 ng/ μL poly dI dC, 10% glycerol, and 20% DMSO. In a volume of 10 μL , 0.1 pmol of FBP was allowed to bind 0.1 pmol of ^{32}P -labeled oligo FMYC 1-6 (d(GATATTCCCTCGGGATTTTT-TATTTTGT)),⁴¹ which includes the FUSE binding site. Dissociation of binding was measured by including either 5 pmol of unlabeled FMYC 1-6 or drug in the mixture. Reactions were incubated at room temperature for 30 min to which 2 μL of dye was added. An amount of 6 μL was added to 8% acrylamide Bis 29:1 gels that were then prerun at 180 V for 1 h followed by running at 180 V for 2 h. Gels were exposed to Kodak XAR film at -80 $^\circ\text{C}$ for 16 h. GST-tagged human RNP K protein was expressed in *E. coli* and purified as described.⁴² By use of 10 μL of buffer described for the FBP experiments, 0.2 pmol of protein was incubated with 0.1 pmol of ^{32}P -labeled Oligo EM 8 (d(AATTCTCCTCCCCACCTTCCCCACCCTCCCCA))⁴² in the presence or absence of 2 pmol of unlabeled oligo or compound. Bound and free oligos were separated on 6% acrylamide Bis 29:1 gels and exposed to Kodak XAR film at room temperature for 1 h. Band intensities for the protein-labeled probe complexes as a function of compound **1** concentration were quantitated by densitometry and fit with a least-squares method to estimate the IC_{50} of compound **1** for each KH domain-containing protein.

Acknowledgment. The authors thank Dr. Ed Olejniczak for many helpful discussions related to this work. These studies were supported in part by the AIDS Targeted Antiviral Program of the Office of the Director of the National Institutes of Health (support to G.M.C.).

Appendix

Abbreviations. ssDNA, single-stranded DNA; NMR, nuclear magnetic resonance; NOE, nuclear Overhauser effect; FBP, far upstream element binding protein; FBP3, KH3 domain of FBP; FBP3/4, construct composed of KH3 and KH4 domains of FBP; SAR, structure-activity relationships; HTS-NMR, high-throughput screening nuclear magnetic resonance spectroscopy; VLS, virtual ligand screening; ASMS, affinity selection/mass spectrometry; HSQC, heteronuclear single quantum correlation.

References

- Grandori, C.; Cowley, S. M.; James, L. P.; Eisenman, R. N. The Myc/Max/Mad network and the transcriptional control of cell behavior. *Annu. Rev. Cell Dev. Biol.* **2000**, *16*, 653-699.
- Jain, M.; Arvanitis, C.; Chu, K.; Dewey, W.; Leonhardt, E.; et al. Sustained loss of a neoplastic phenotype by brief inactivation of MYC. *Science* **2002**, *297*, 102-104.
- Park, J.; Wood, M. A.; Cole, M. D. BAF53 Forms Distinct Nuclear Complexes and Functions as a Critical c-Myc-Interacting Nuclear Cofactor for Oncogenic Transformation. *Mol. Cell. Biol.* **2002**, *22*, 1307-1316.

- (4) Liu, J.; He, L.; Collins, I.; Ge, H.; Libutti, D.; et al. The FBP interacting repressor targets TFIID to inhibit activated transcription. *Mol. Cell* **2000**, *5*, 331–341.
- (5) He, L.; Liu, J.; Collins, I.; Sanford, S.; O'Connell, B.; et al. Loss of FBP function arrests cellular proliferation and extinguishes *c-myc* expression. *EMBO J.* **2000**, *19*, 1034–1044.
- (6) Duncan, R. C.; Bazar, L.; Michelotti, G.; Tomonaga, T.; Krutsch, H.; et al. A sequence-specific, single strand binding protein activates the far-upstream of *c-myc* and defines a new DNA binding motif. *Genes Dev.* **1994**, *8*, 465–480.
- (7) Michelotti, G. A.; Michelotti, E. F.; Pulner, A.; Duncan, R. C.; Eick, D.; et al. Multiple single-stranded cis elements are associated with activated chromatin of the human *c-myc* gene in vivo. *Mol. Cell Biol.* **1996**, *16*, 2656–2669.
- (8) Kim, M. J.; Park, B.-J.; Kang, Y.-S.; Kim, H. J.; Park, J.-H.; et al. Downregulation of FUSE-binding protein and *c-myc* by tRNA synthetase cofactor p38 is required for lung cell differentiation. *Nat. Genet.* **2003**, *34*, 330–336.
- (9) Liu, J.; Akoulitchev, S.; Weber, A.; Ge, H.; Chuikov, S.; et al. Defective Interplay of Activators and Repressors with TFIID in Xeroderma Pigmentosa. *Cell* **2001**, *104*, 353–363.
- (10) Braddock, D. T.; Louis, J. M.; Baber, J. L.; Levens, D.; Clore, G. M. Structure and dynamics of KH domains from FBP bound to single-stranded DNA. *Nature* **2002**, *415*, 1051–1056.
- (11) Mrksich, M.; Parks, M. E.; Dervan, P. B. A new class of oligopeptides for sequence-specific recognition in the minor groove of double helical DNA. *J. Am. Chem. Soc.* **1994**, *116*, 7983–7988.
- (12) Hajduk, P. J.; Gerfin, T.; Boehlen, J. M.; Haberli, M.; Marek, D.; et al. High-throughput nuclear magnetic resonance-based screening. *J. Med. Chem.* **1999**, *42*, 2315–2317.
- (13) McGann, M. R.; Almond, H. R.; Nicholls, A.; Grant, J. A.; Brown, F. K. Gaussian Docking Functions. *Biopolymers* **2003**, *68*, 76–90.
- (14) Qian, J.; Voorbach, M. J.; Huth, J. R.; Coen, M. L.; Zhang, H.; et al. Discovery of novel inhibitors of Bcl-xL using multiple high-throughput screening platforms. *Anal. Biochem.* **2004**, *328*, 131–138.
- (15) Falb, D.; Jindal, S. Chemical genomics: bridging the gap between the proteome and therapeutics. *Curr. Opin. Drug Discovery Dev.* **2002**, *5*, 532–539.
- (16) Muckenschnabel, I.; Falchetto, R.; Mayr, L. M.; Filipuzzi, I. SpeedScreen: label-free liquid chromatography–mass spectrometry-based high-throughput screening for the discovery of orphan protein ligands. *Anal. Biochem.* **2004**, *324*, 241–249.
- (17) Braddock, D. T.; Baber, J. L.; Levens, D.; Clore, G. M. Molecular basis of sequence-specific single-stranded DNA recognition by KH domains: solution structure of a complex between hnRNP K KH3 and single-stranded DNA. *EMBO J.* **2002**, *21*, 3476–3485.
- (18) Gadek, T. R. Strategies and methods in the identification of antagonists of protein–protein interactions. *Biotechniques* **2003**, June (Suppl.), 21–24.
- (19) Lugovskoy, A. A.; Degterev, A. I.; Fahmy, A. F.; Zhou, P.; Gross, J. D.; et al. A novel approach for characterizing protein ligand complexes: molecular basis for specificity of small-molecule Bcl-2 inhibitors. *J. Am. Chem. Soc.* **2002**, *124*, 1234–1240.
- (20) Kuruvilla, F. G.; Shamji, A. F.; Sternson, S. M.; Hergenrother, P. J.; Schreiber, S. L. Dissecting glucose signalling with diversity-oriented synthesis and small-molecule microarrays. *Nature* **2002**, *416*, 653–657.
- (21) Hajduk, P. J.; Dinges, J.; Miknis, G. F.; Merlock, M.; Middleton, T.; et al. NMR-based discovery of lead inhibitors that block DNA binding of the human papillomavirus e2 protein. *J. Med. Chem.* **1997**, *40*, 3144–3150.
- (22) Thanos, C. D.; Randal, M.; Wells, J. A. Potent small-molecule binding to a dynamic hot spot on IL-2. *J. Am. Chem. Soc.* **2003**, *125*, 15280–15281.
- (23) Devlin, J. P. Chemical Diversity and Genetic Equity: Synthetic and Naturally Derived Compounds. *High Throughput Screening: The Discovery of Bioactive Substances*, Marcel Dekker: New York, 1997; pp 4–5.
- (24) Archakov, A. I.; Govorun, V. M.; Dubanov, A. V.; Ivanov, Y. D.; Veselovsky, A. V.; et al. Protein–protein interactions as a target for drugs in proteomics. *Proteomics* **2003**, *3*, 380–391.
- (25) Bogan, A. A.; Thorn, K. S. Anatomy of hot spots in protein interfaces. *J. Mol. Biol.* **1998**, *280*, 1–9.
- (26) Toogood, P. L. Inhibition of Protein–Protein Association by Small Molecules: Approaches and Progress. *J. Med. Chem.* **2002**, *45*, 1543–1558.
- (27) Shuker, S. B.; Hajduk, P. J.; Meadows, R. P.; Fesik, S. W. Discovering high-affinity ligands for proteins—SAR by NMR. *Science* **1996**, *274*, 1531–1534.
- (28) Hajduk, P. J.; Meadows, R. P.; Fesik, S. W. Discovering high-affinity ligands for proteins. *Science* **1997**, *278*, 497–499.
- (29) Huth, J. R.; Sun, C. Utility of NMR in lead optimization: fragment-based approaches. *Comb. Chem. High Throughput Screening* **2002**, *5*, 631–643.
- (30) Dervan, P. B.; Edelson, B. S. Recognition of the DNA minor groove by pyrrole-imidazole polyamides. *Curr. Opin. Struct. Biol.* **2003**, *13*, 284–299.
- (31) Gottesfeld, J. M.; Neely, L.; Trauger, J. W.; Baird, E. E.; Dervan, P. B. Regulation of gene expression by small molecules. *Nature* **1997**, *387*, 202–205.
- (32) Hajduk, P. J.; Augeri, D. J.; Mack, J.; Mendoza, R.; Yang, J. G.; et al. NMR-based screening of proteins containing C-13-labeled methyl groups. *J. Am. Chem. Soc.* **2000**, *122*, 7898–7904.
- (33) Clore, G. M.; Gronenborn, A. M. Determining the structures of large proteins and protein complexes by NMR. *Trends Biotechnol.* **1998**, *16*, 22–34.
- (34) Hajduk, P. J.; Sheppard, G.; Nettlesheim, D. G.; Olejniczak, E. T.; Shuker, S. B.; et al. Discovery of potent nonpeptide inhibitors of stromelysin using SAR by NMR. *J. Am. Chem. Soc.* **1997**, *119*, 5818–5827.
- (35) Baxter, C. A.; Murray, C. W.; Clark, D. E.; Westhead, D. R.; Eldridge, M. D. Flexible docking using Tabu search and an empirical estimate of binding affinity. *Proteins* **1998**, *33*, 367–382.
- (36) Stahl, M.; Rarey, M. Detailed Analysis of Scoring Functions for Virtual Screening. *J. Med. Chem.* **2001**, *44*, 1035–1042.
- (37) Clore, G. M.; Gronenborn, A. M. Structures of larger proteins in solution: three- and four-dimensional heteronuclear NMR spectroscopy. *Science* **1991**, *252*, 1390–1399.
- (38) Fesik, S. W.; Zuiderweg, E. R. P. Heteronuclear Three-Dimensional NMR Spectroscopy. A Strategy for the Simplification of Homonuclear Two-Dimensional NMR Spectra. *J. Magn. Reson.* **1988**, *78*, 588–593.
- (39) Schwieters, C. D.; Clore, G. M. Internal coordinates for molecular dynamics and minimization in structure determination and refinement. *J. Magn. Reson.* **2001**, *152*, 288–302.
- (40) Schwieters, C. D.; Clore, G. M. The VMD-XPLOR visualization package for NMR structure refinement. *J. Magn. Reson.* **2001**, *149*, 239–244.
- (41) Davis-Smyth, T.; Duncan, R. C.; Zheng, T.; Michelotti, G.; Levens, D. The far upstream element-binding proteins comprise an ancient family of single-strand DNA-binding transactivators. *J. Biol. Chem.* **1996**, *271*, 31679–31687.
- (42) Tomonaga, T.; Levens, D. Heterogeneous nuclear ribonucleoprotein K is a DNA-binding transactivator. *J. Biol. Chem.* **1995**, *270*, 4875–4881.
- (43) Li, Z.; Van Calcar, S.; Qu, C.; Cavenee, W. K.; Zhang, M. Q.; et al. A global transcriptional regulatory role for c-Myc in Burkitt's lymphoma cells. *Proc. Natl. Acad. Sci. U.S.A.* **2003**, *100*, 8164–8169.

JM0497803